SUPPLEMENTAL METHODS

Optimization of Region of Interest for Input Function

For the region-of-interest (ROI) method, myocardial images were generated from later frames after 2 min. The ROI was then positioned in the short axis in the middle of the left ventricle as a square with a width of 2 pixels to minimize myocardial spillover and positioned in the long axis to include the maximum blood pool activity in the left ventricular (LV) cavity, base, and left atrium, consistent with prior studies (*1*–*4*). The arterial input function obtained from LV ROIs in this manner has been shown to agree closely with directly sampled arterial blood (*5*,*6*). An example of regions used for input function estimation for each of these 3 methods is shown in Supplemental Figure 10. There were notable differences in the input function curves generated by the methods (Supplemental Fig. 10). Generally, the peak height and area under the curve for the ROI method were lower than for the factor analysis and hybrid methods.

SUPPLEMENTAL RESULTS

Evaluation of Effect of Right Ventricular (RV) Spillover Correction

Because RV spillover correction was used when the input function was determined with the factor analysis and hybrid methods and not with the ROI method, we conducted a sensitivity analysis in order to evaluate the impact of this difference on our findings. Myocardial blood flow (MBF) and myocardial flow reserve (MFR) were recomputed for the factor analysis and hybrid methods, omitting RV spillover correction for each of the extraction models used in the primary analysis. We found that stress MBF and MFR estimates computed with and without RV spillover correction were highly correlated (Pearson ρ 0.977 – 0.997, P<0.0001) (Supplemental Fig. 12). Furthermore, distributions of stress MBF and MFR were similar to those without RV spillover correction (Supplemental Figs. 13 & 14). Importantly, there was considerably less variability in MFR estimates than in stress MBF across the various extraction models for ^{82}Rb, particularly when the ROI method was used.

Patterns of correlations between stress MBF estimates and MFR estimates were also similar to the primary analysis, with strong correlations between estimates obtained using the same method for input function estimation and weaker correlations between estimates obtained with the ROI method when compared with estimates obtained with the hybrid or factor analysis methods (Supplemental Figs. 15 & 16). Likewise, patterns of bias between stress MBF and MFR estimates were similar to the primary analysis (Supplemental Figs. 17 & 18), with consistently large biases between measures obtained with different input function estimation methods. Consistency of MFR estimates across clinically relevant categories of <1.5, 1.5-2.0 and >2.0 was also similar to the primary analysis (Supplemental Fig. 19).

Most importantly, risk of cardiac death across stress MBF and MFR ranges was largely unchanged compared with the primary analysis (Supplemental Figs. 20 & 21). The pattern of increased risk with reduced MFR <2.0 was seen regardless of input function estimation method and ^{82}Rb extraction model used. As in the primary analysis, much greater variability was noted in the relationship between stress MFR and cardiac death, particularly when the ROI method was used.

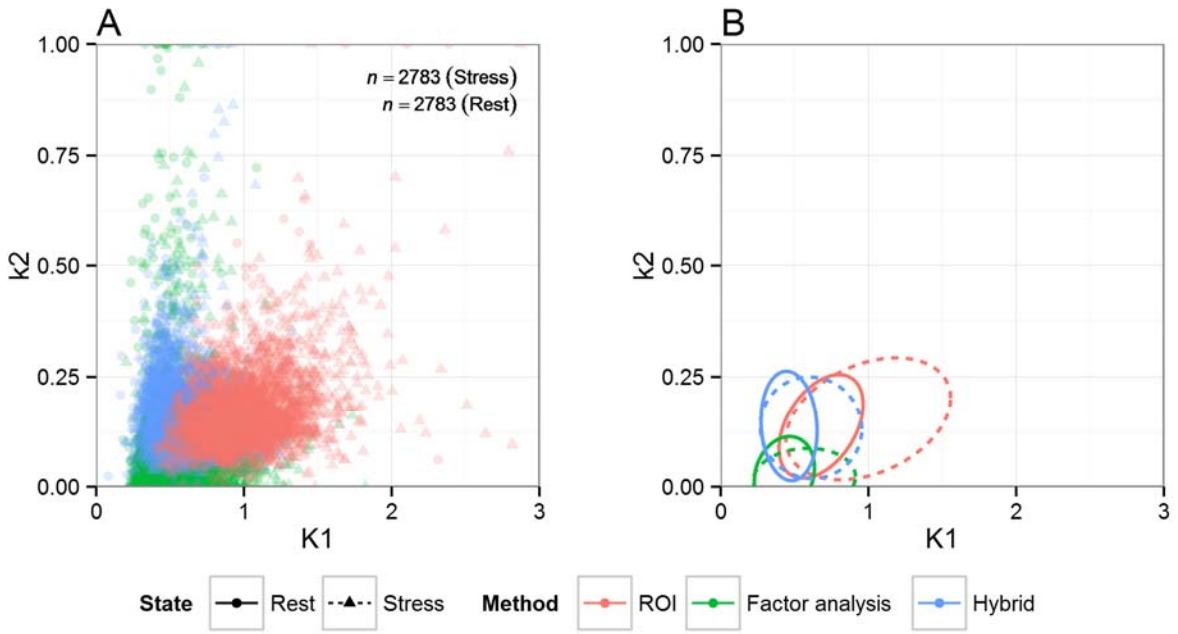

Supplemental Figure 1: Variability in K_1 and k_2 Estimates by Input Function Method. Scatter plot (A) of the estimated K_1 and k_2 rate constants at stress and rest colored by method of input function determination. The 3 methods each fall into distinct clusters, although some overlap exists. 95% confidence ellipses for K_1 and k_2 for all input function determinations methods at rest (solid lines) and stress (dashed lines) (B).

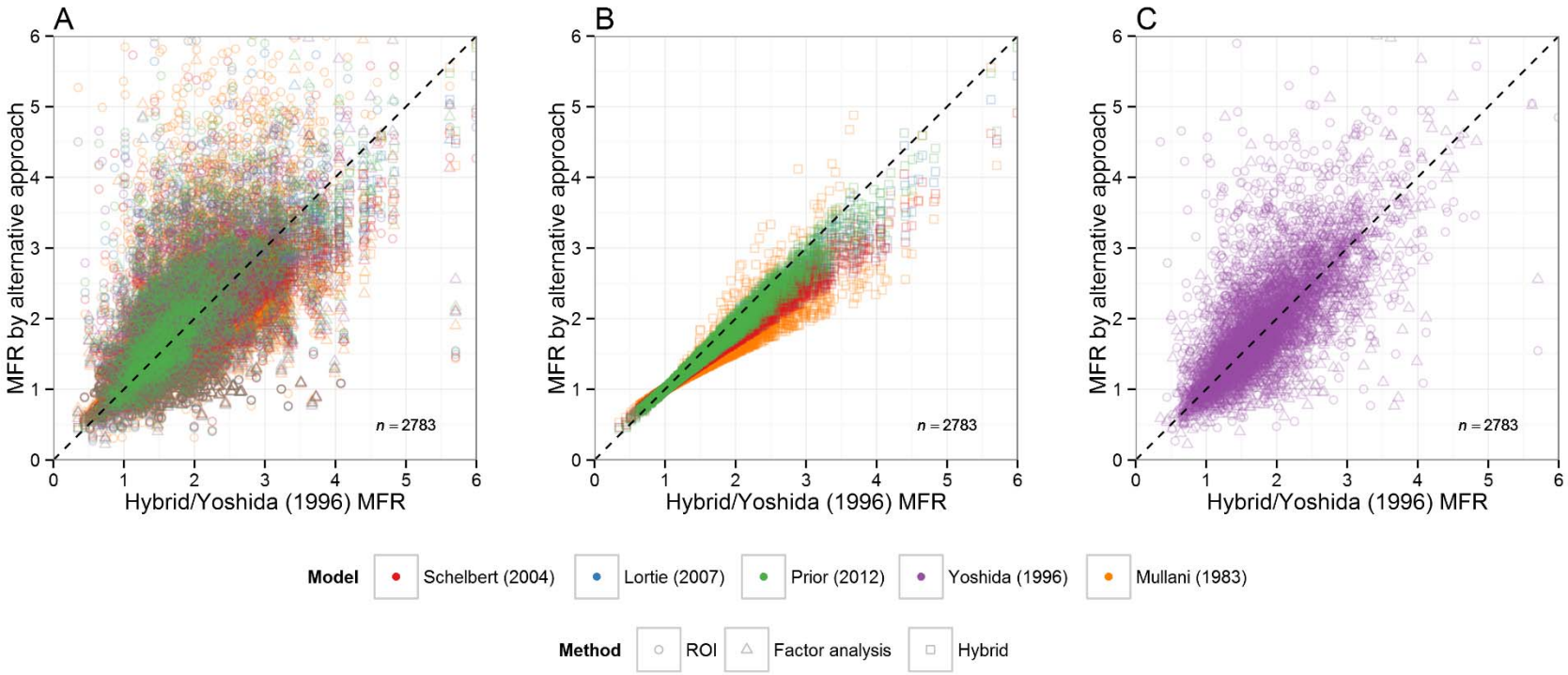

Supplemental Figure 2: Comparison of MFR with Different Input Function Methods and Extraction Models. Correlation of MFR estimates obtained with the ROI, factor analysis and hybrid methods for estimation of the input function and 5 extraction models for ^{82}Rb with the combination of the hybrid method and the Yoshida et al. (*2*) extraction model. There is wide scatter and limited overall correlation across MFR estimates (A). However, when only the hybrid method is used, all 5 extraction models result in similar flows, which are closely correlated (B). In contrast, when the Yoshida et al. extraction model is coupled with other methods for input function estimation, correlation with the hybrid method is limited, particularly for the ROI method (C).

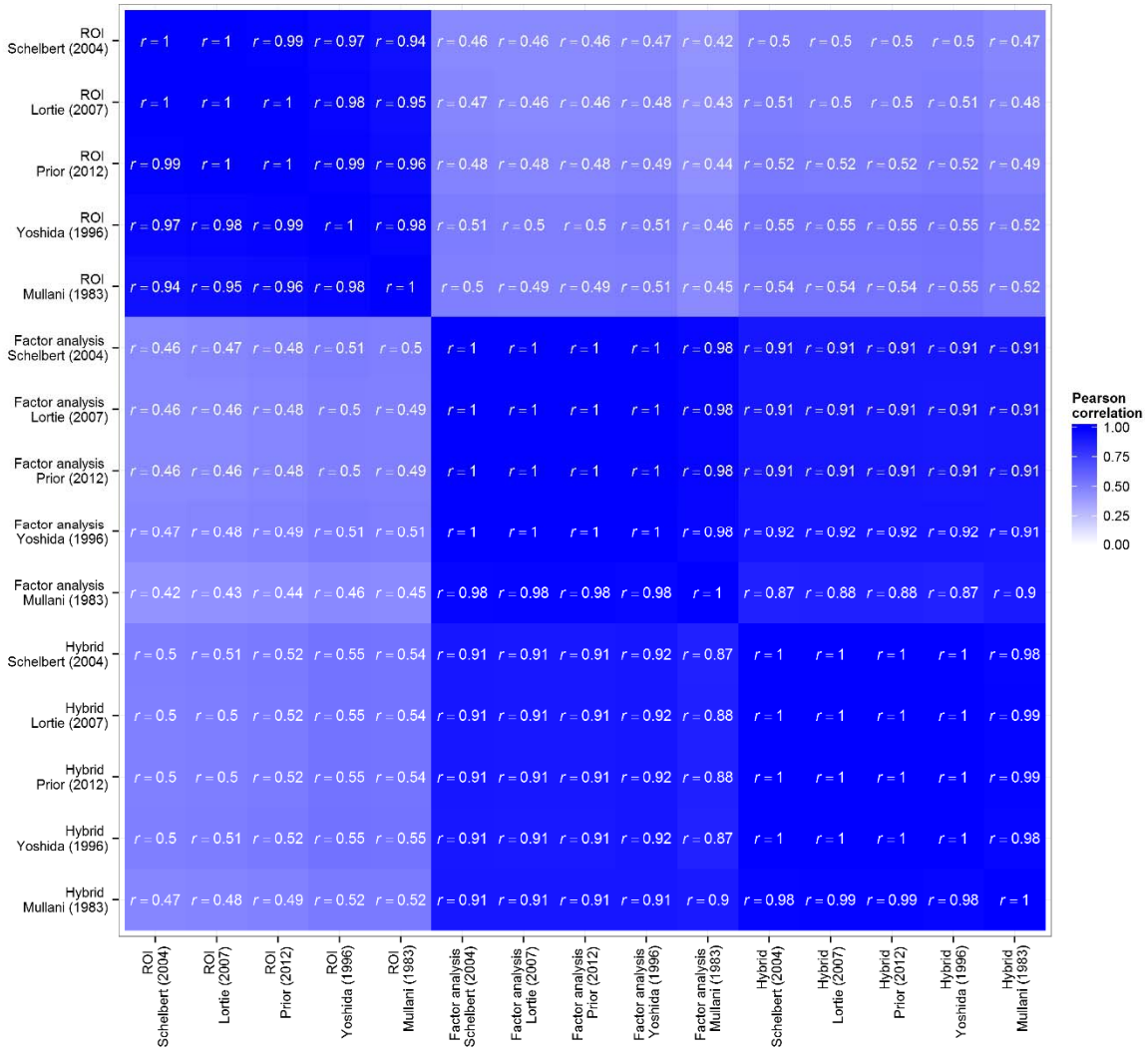

Supplemental Figure 3: Pearson Correlations for Stress MBF Measures.

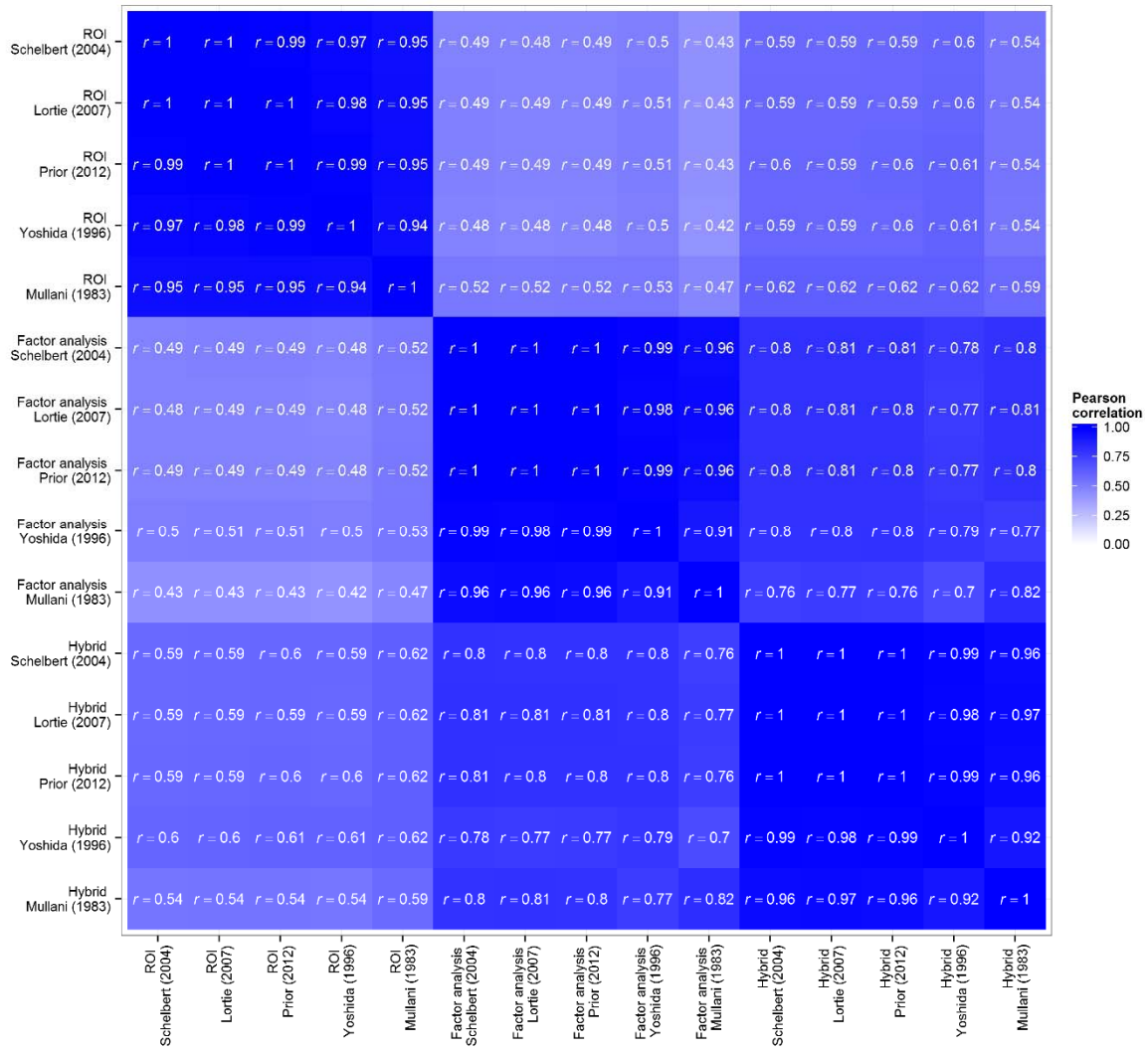

Supplemental Figure 4: Pearson Correlations for MFR Measures.

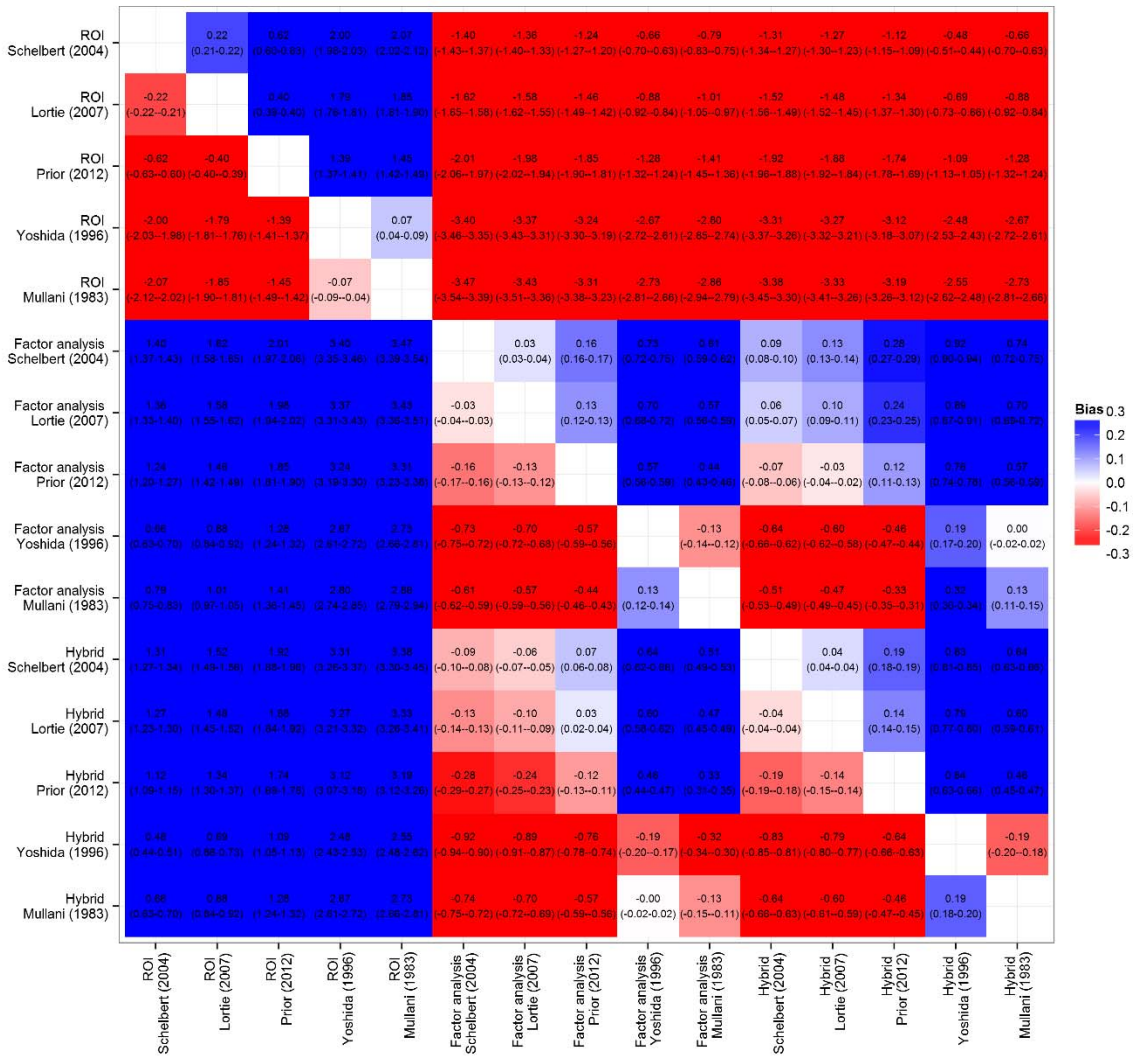

Supplemental Figure 5: Bias Estimates for Stress MBF.

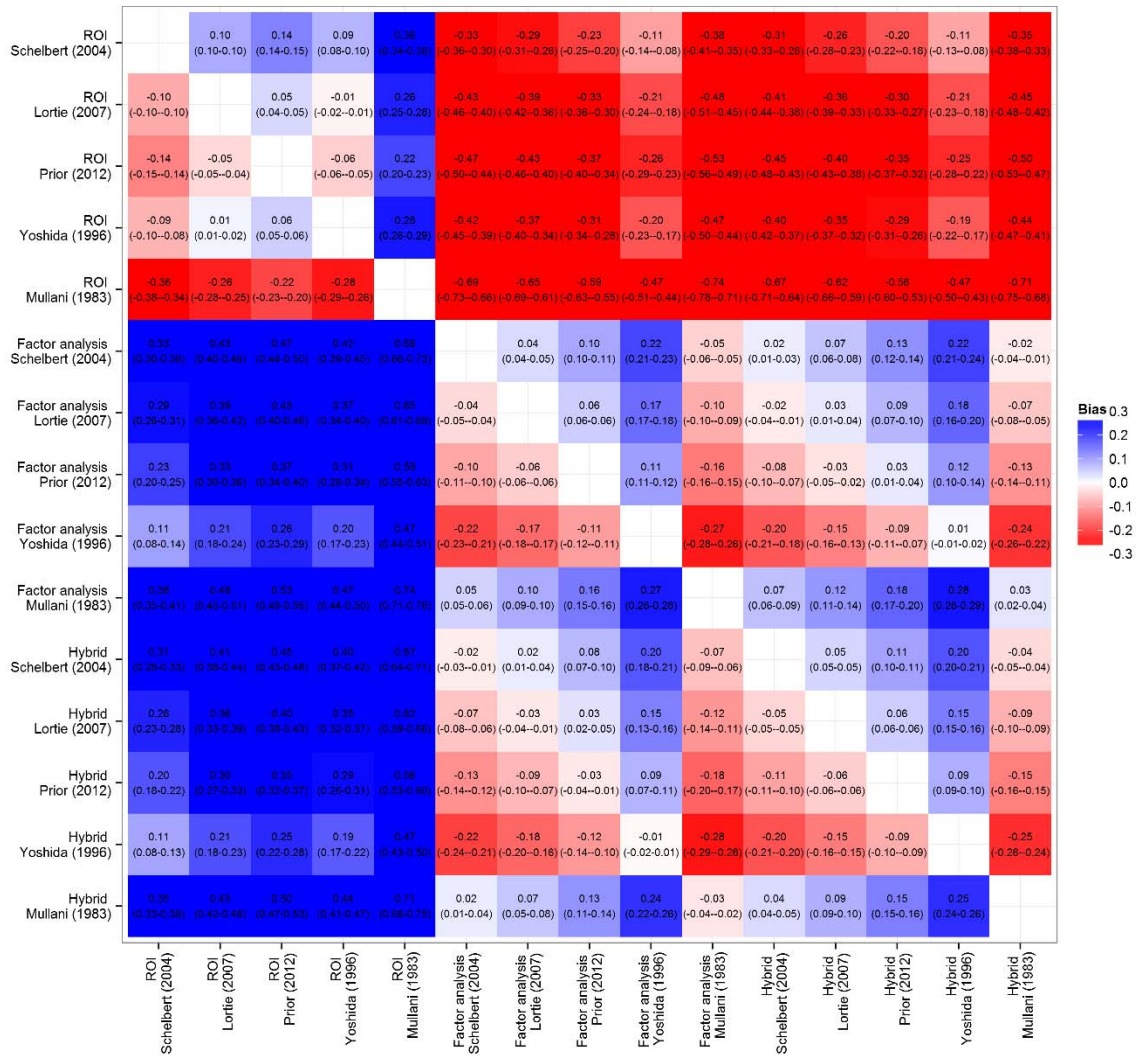

Supplemental Figure 6: Bias Estimates for MFR.

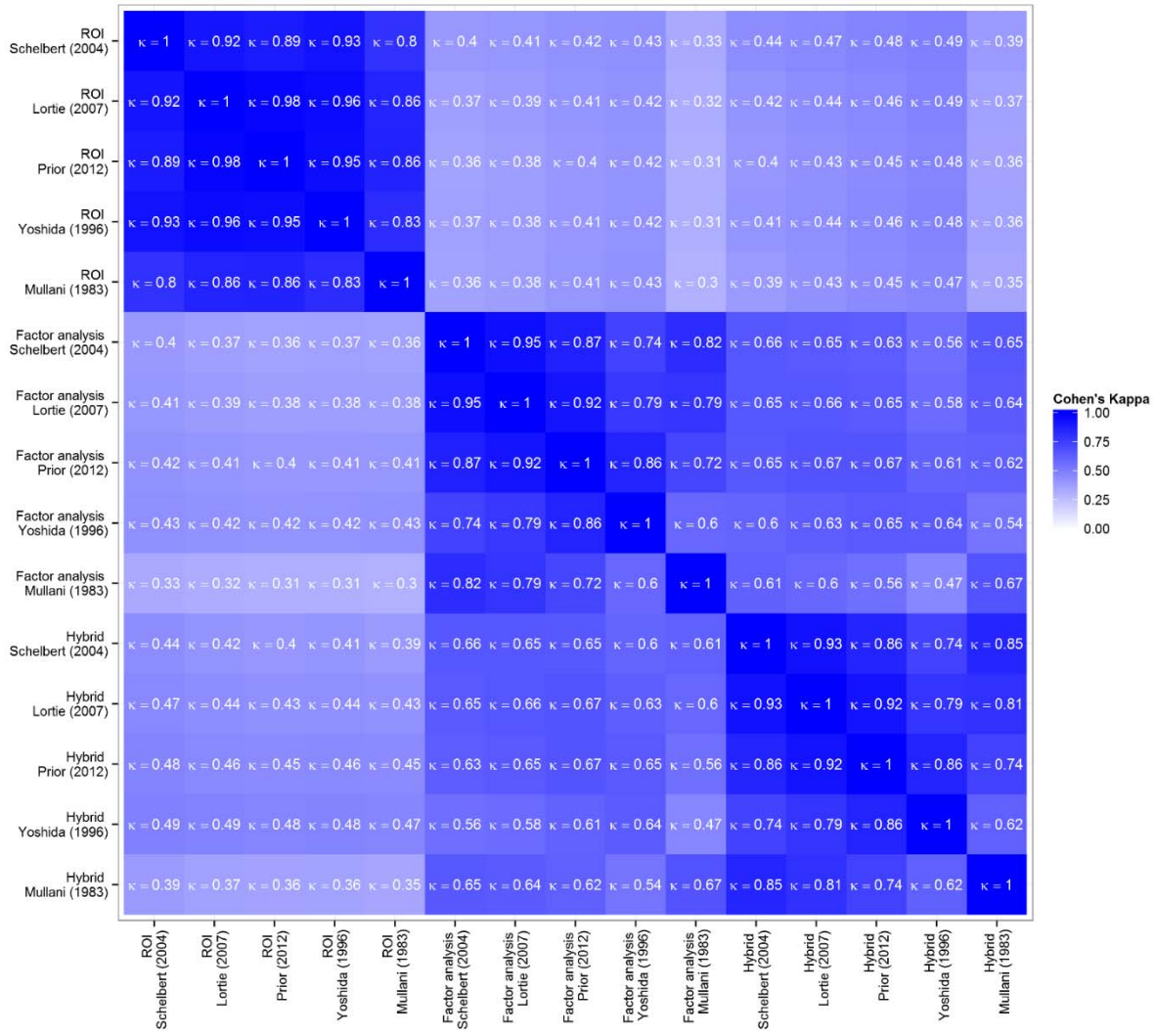

Supplemental Figure 7: Cohen's Kappa for MFR.

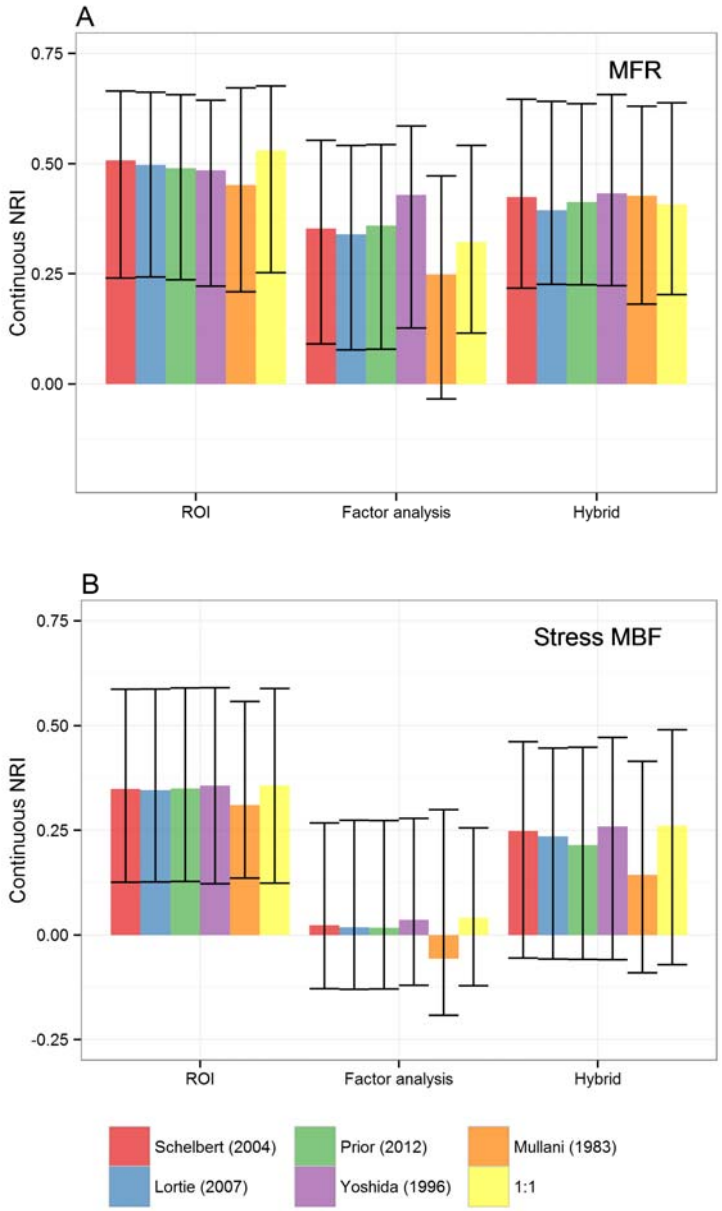

Supplemental Figure 8: Net Reclassification Improvement for Cardiac Death by MFR and Stress MBF. Continuous net reclassification improvement (NRI) for addition of (A) MFR or (B) stress MBF to a Cox proportional hazard model containing age, gender, hypertension, dyslipidemia, diabetes, smoking, family history of coronary artery disease (CAD), prior CAD, body mass index (BMI), chest pain, dyspnea, early revascularization (<90 days), left ventricular ejection fraction

(LVEF), and stress-induced augmentation of LVEF. Stress MBF and MFR were computed using 1 of 3 input function estimation methods (ROI, factor analysis and a hybrid method) and 1 of 5 clinically used extraction models for ^{82}Rb and a counterfactual model assuming 100% extraction (1:1). Because MFR and stress MBF are modeled as linear predictors, these estimates may substantially understate their impact.

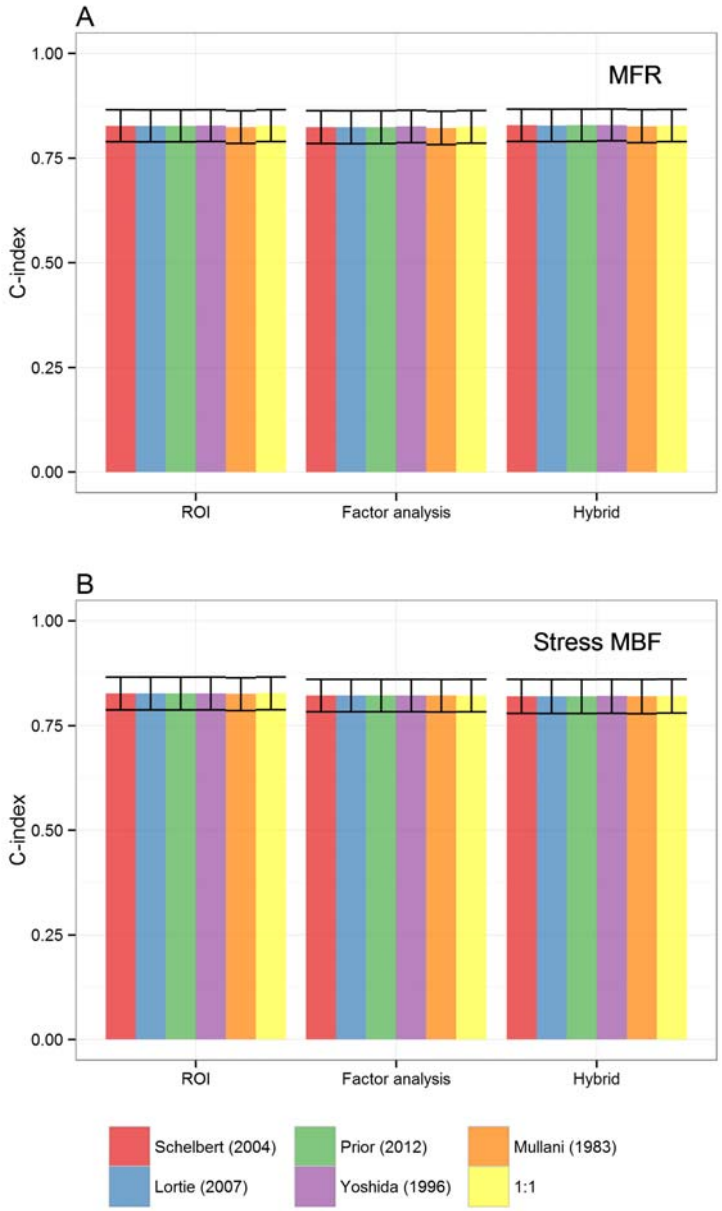

Supplemental Figure 9: C-Indices. C-indices for addition of (A) MFR or (B) stress MBF to a Cox proportional hazard model containing age, gender, hypertension, dyslipidemia, diabetes, smoking, family history of coronary artery disease (CAD), prior CAD, body mass index (BMI), chest pain, dyspnea, early revascularization (<90 days), left ventricular ejection fraction (LVEF), and stress-induced augmentation of LVEF. Stress MBF and MFR

were computed using one of 3 input function estimation methods (ROI, factor analysis and a hybrid method) and 1 of 5 clinically used extraction models for ^{82}Rb and a counterfactual model assuming 100% extraction (1:1). Because MFR and stress MBF are modeled as linear predictors, these estimates may substantially understate their impact.

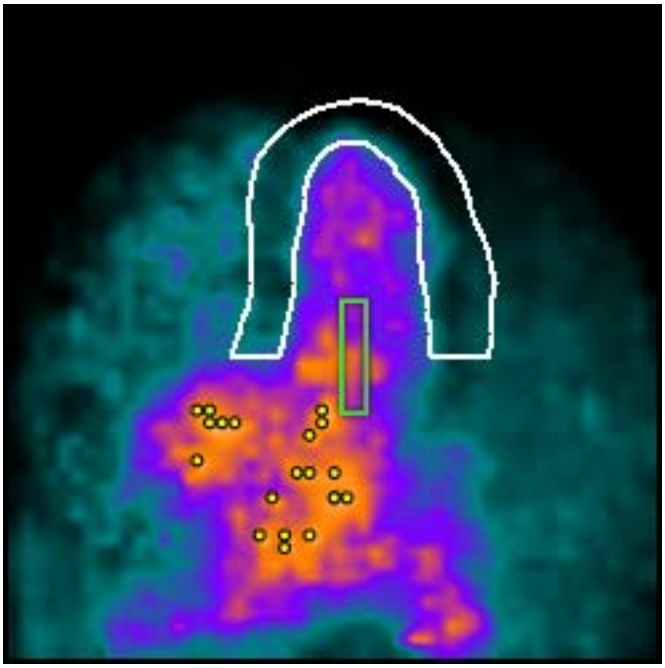

Supplemental Figure 10: Comparison of Input Function Determination Methods. Maximum-intensity projection of image regions used to estimate the input function. The ROI method is indicated as a green rectangle. The factor analysis method uses the entire LV blood pool factor, indicated as the multicolor region. The hybrid method uses the 20 highest intensity pixels within the LVar factor (yellow circles). The LV myocardial contours are indicated in white.

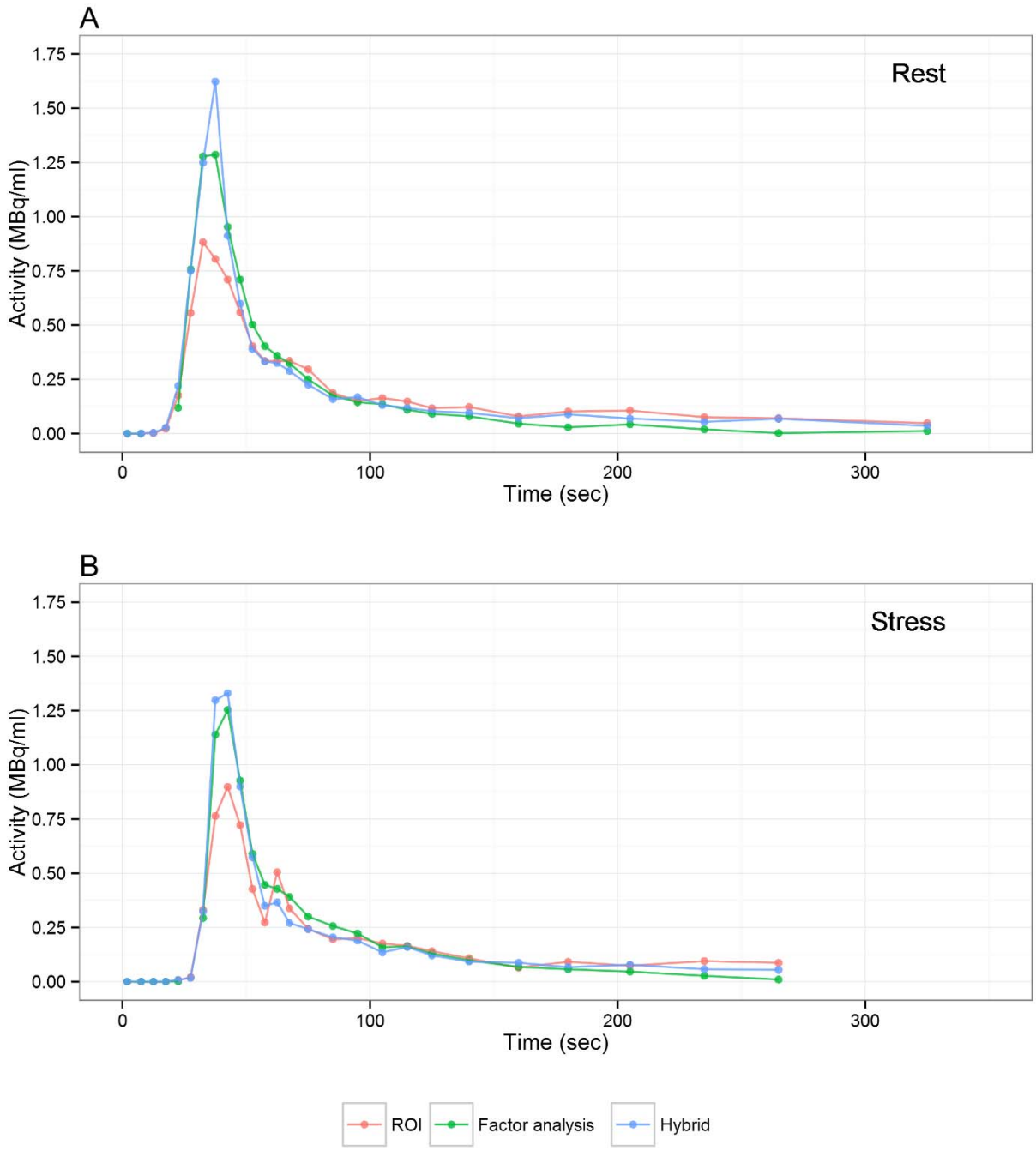

Supplemental Figure 11: Comparison of Input Function Time Activity Curves. LV blood-pool input functions estimated with ROI, factor analysis and hybrid methods for a representative patient example at rest (A) and stress (B). Of note, the peak heights and areas under the curve are consistently lower for the ROI method than for the other 2 methods.

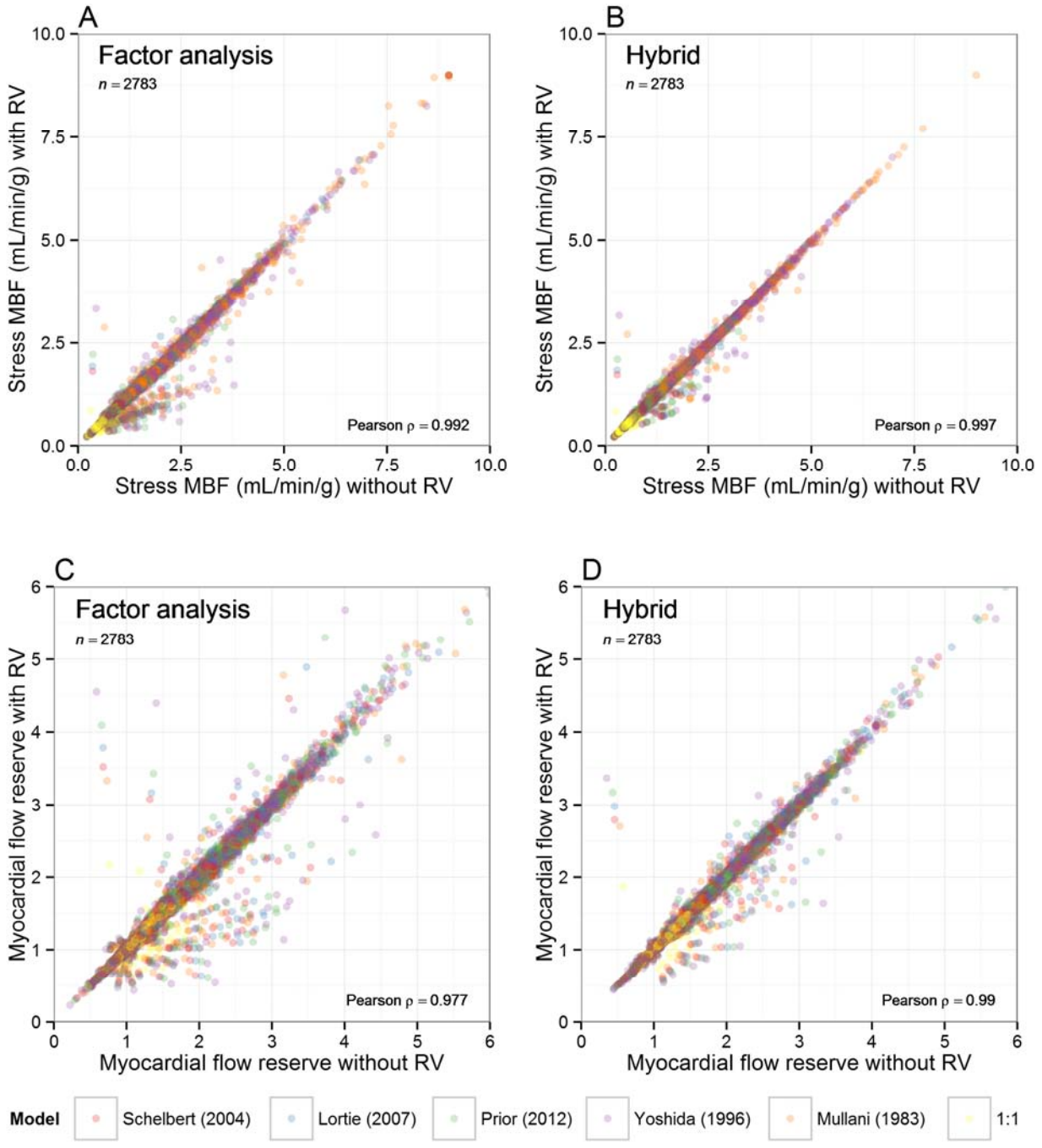

Supplemental Figure 12: Comparison of Stress MBF and MFR Estimates With and Without RV Spillover Correction. Stress MBF (A and B) and MFR (C and D) are highly correlated whether RV spillover correction was or was not applied for both the factor analysis (A and C) and hybrid (B

and D) methods for estimation of the input function across 5 different clinically used extraction models for ^{82}Rb and a counterfactual model assuming 100% extraction (1:1).

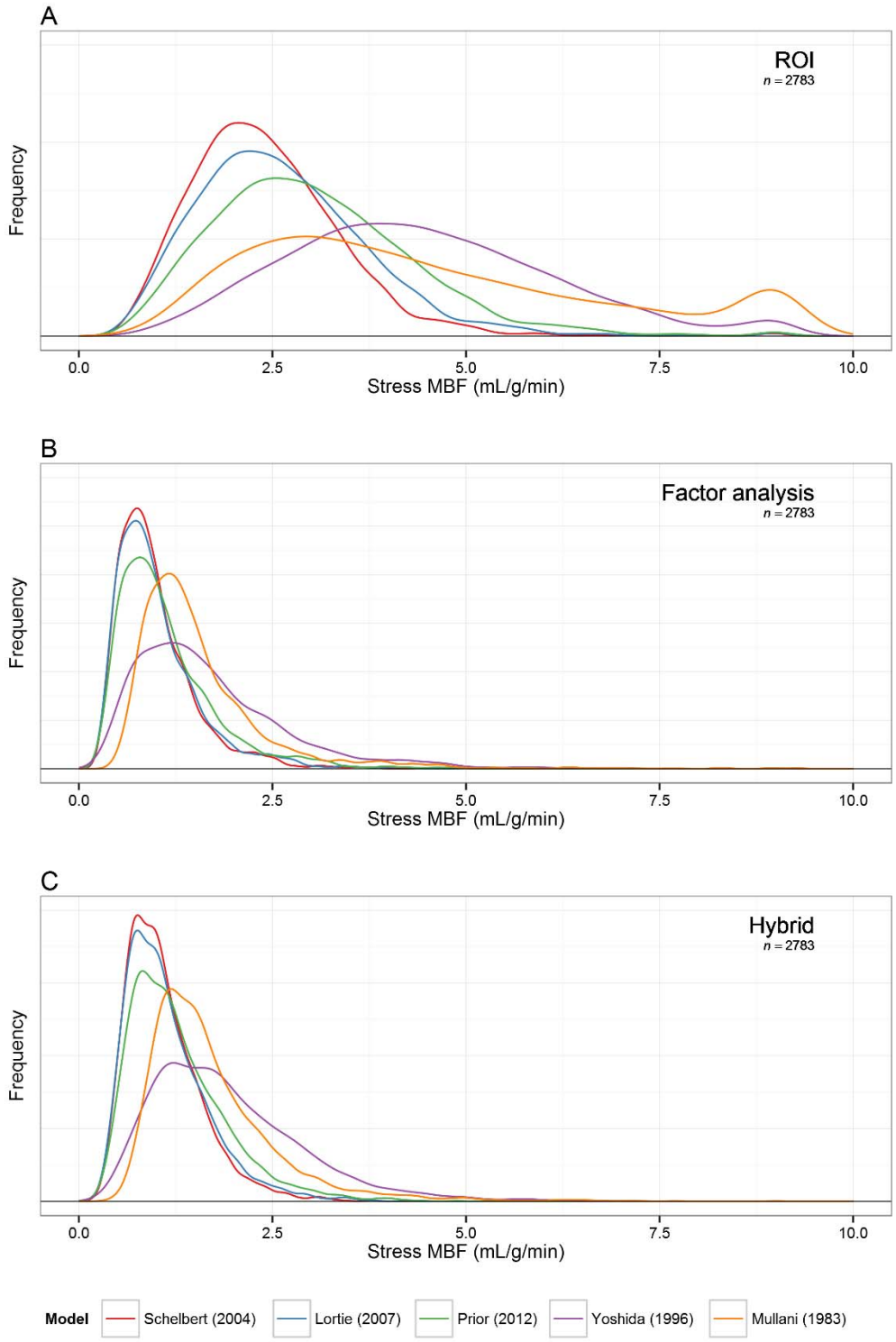

Supplemental Figure 13: Distribution of Stress MBF by Input Function Method and ^{82}Rb Extraction Model Without RV Spillover Correction. Distribution of stress MBF estimates using

(A) ROI, (B) factor analysis, and (C) hybrid methods for estimation of the input function and 5 different clinically used extraction models. For this analysis no RV spillover correction was performed for any of the input function methods. In contrast, in Figure 2, RV spillover correction was performed for the factor analysis and hybrid methods.

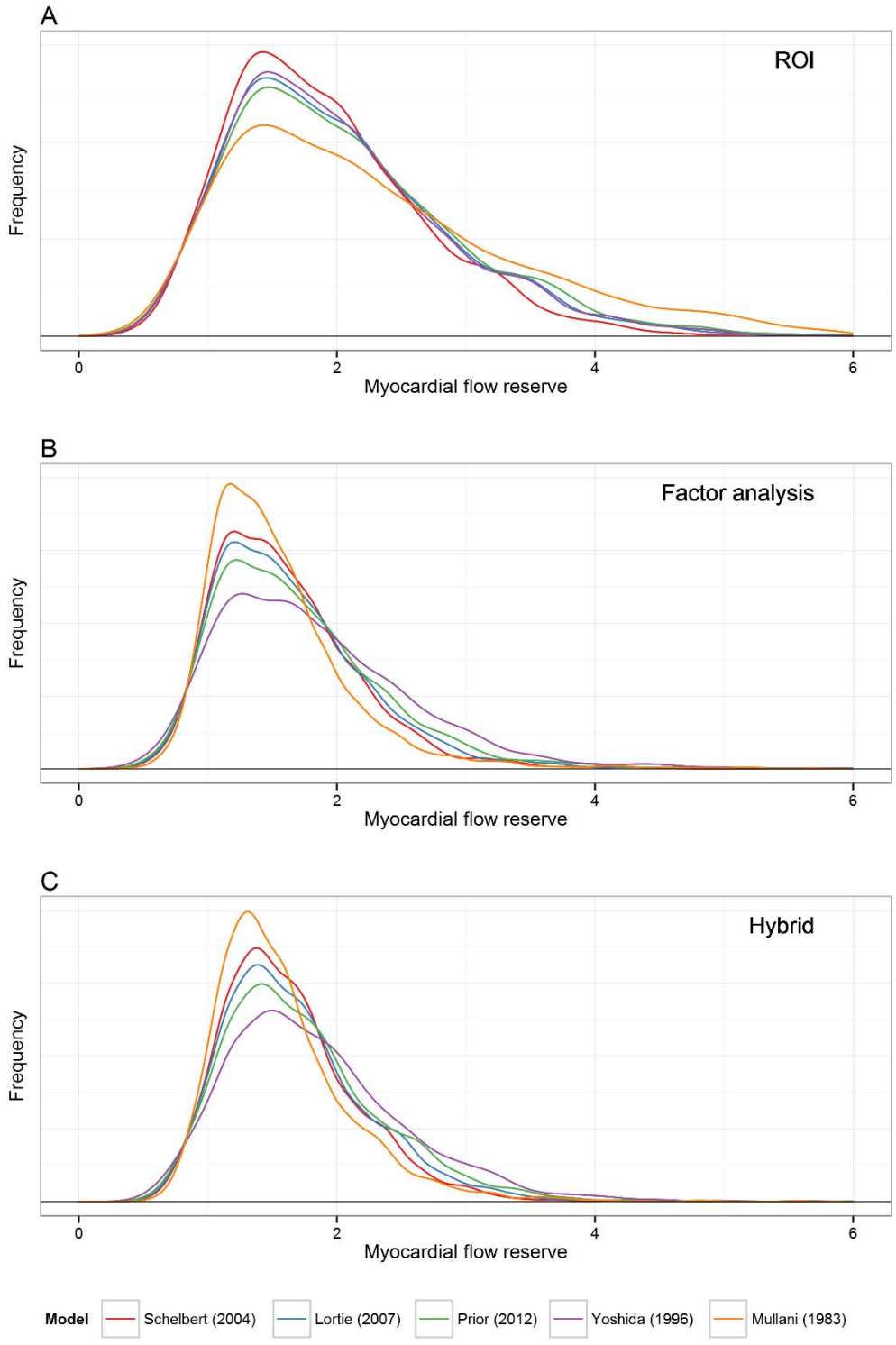

Supplemental Figure 14: Distribution of MFR by Input Function Method and ^{82}Rb Extraction Model Without RV Spillover Correction. Distribution of MFR estimates using (A) ROI, (B) factor

analysis, and (C) hybrid methods for estimation of the input function and 5 different clinically used extraction models. For this analysis no RV spillover correction was performed for any of the input function methods. In contrast, in Figure 3, RV spillover correction was performed for the factor analysis and hybrid methods.

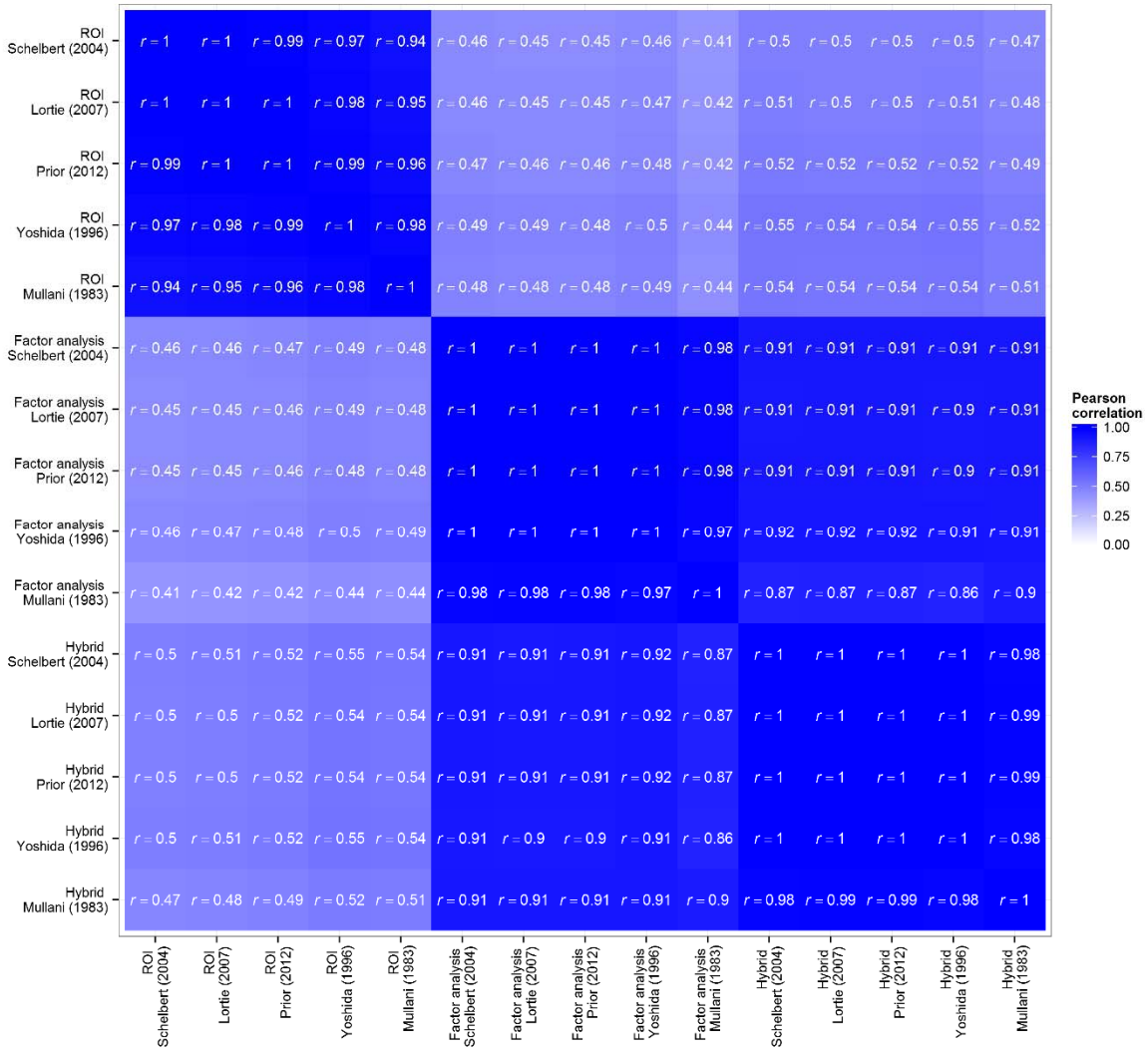

Supplemental Figure 15: Pearson Correlations for Stress MBF Measures Without RV Spillover Correction.

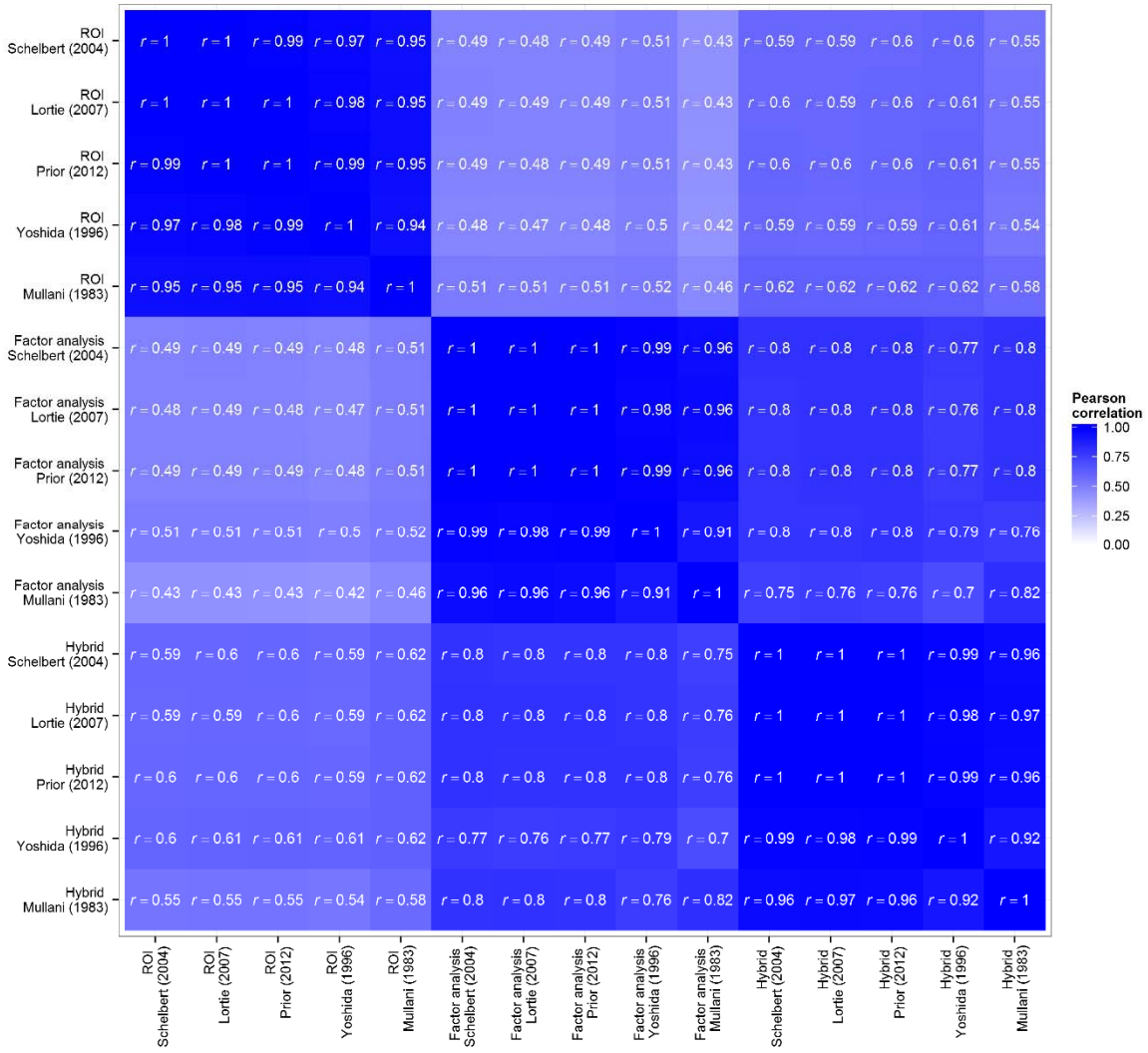

Supplemental Figure 16: Pearson Correlations for MFR Measures Without RV Spillover Correction.

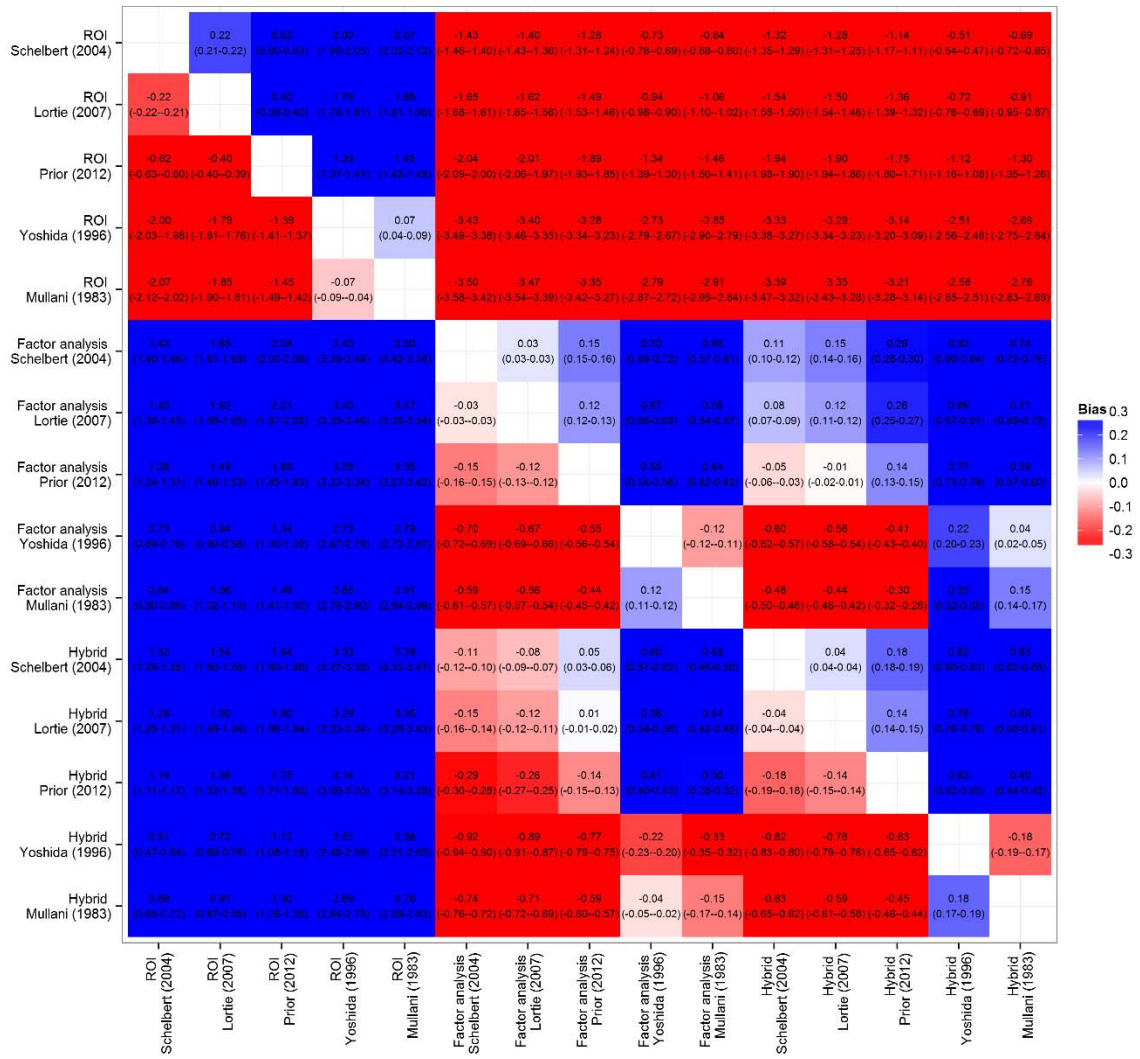

Supplemental Figure 17: Bias Estimates for Stress MBF Without RV Spillover Correction.

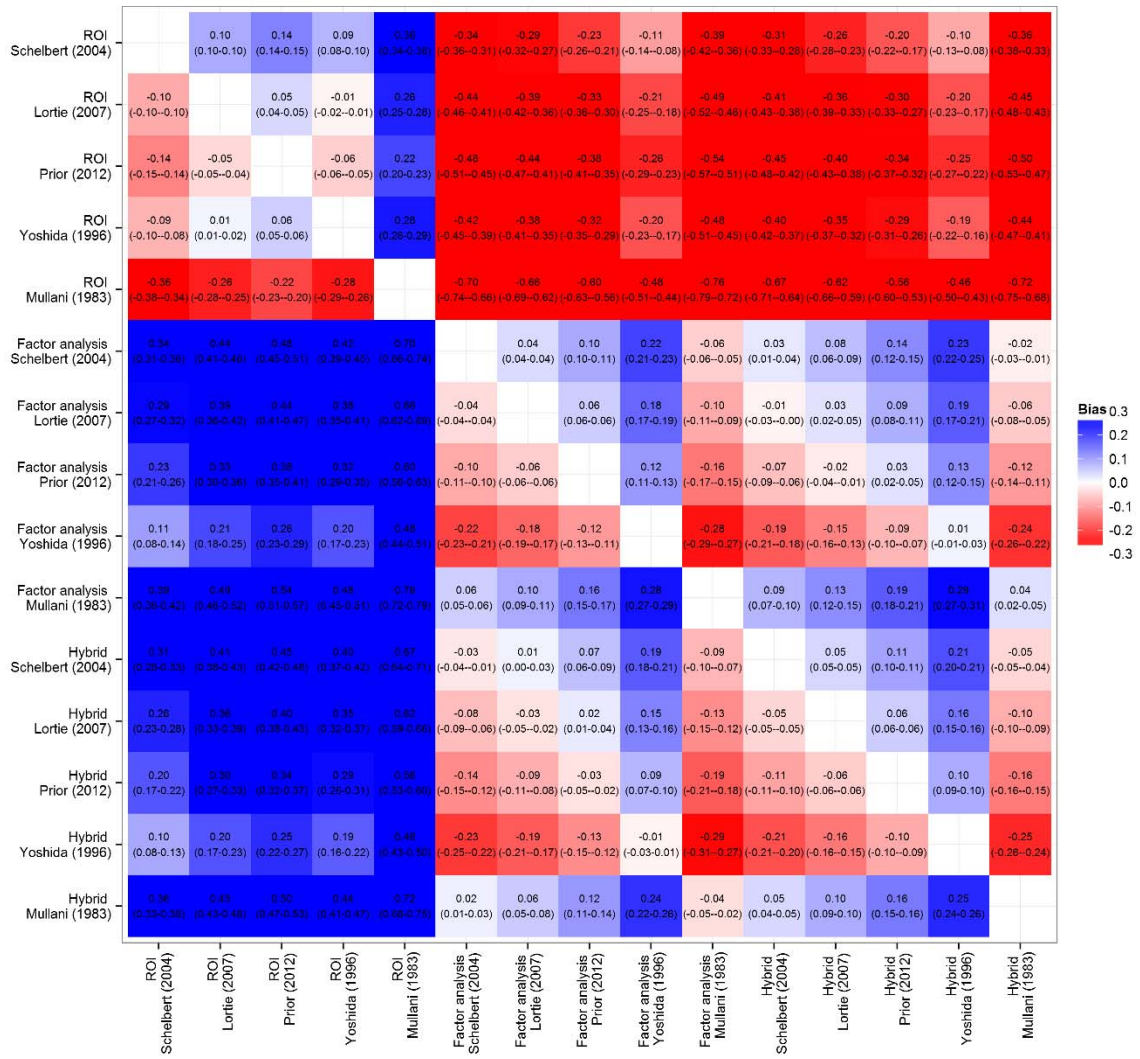

Supplemental Figure 18: Bias Estimates for MFR Without RV Spillover Correction.

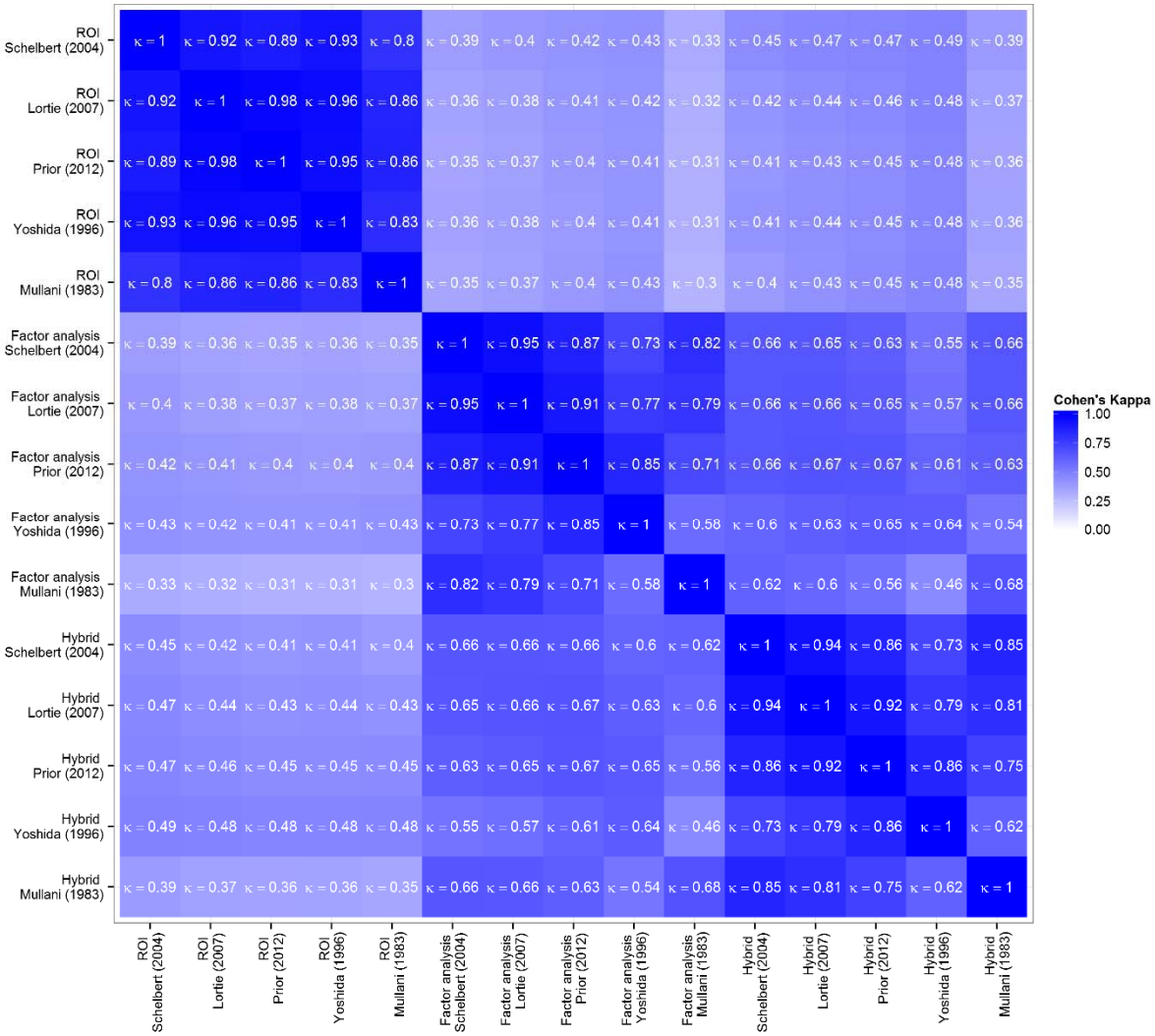

Supplemental Figure 19: Cohen's Kappa for MFR Without RV Spillover Correction.

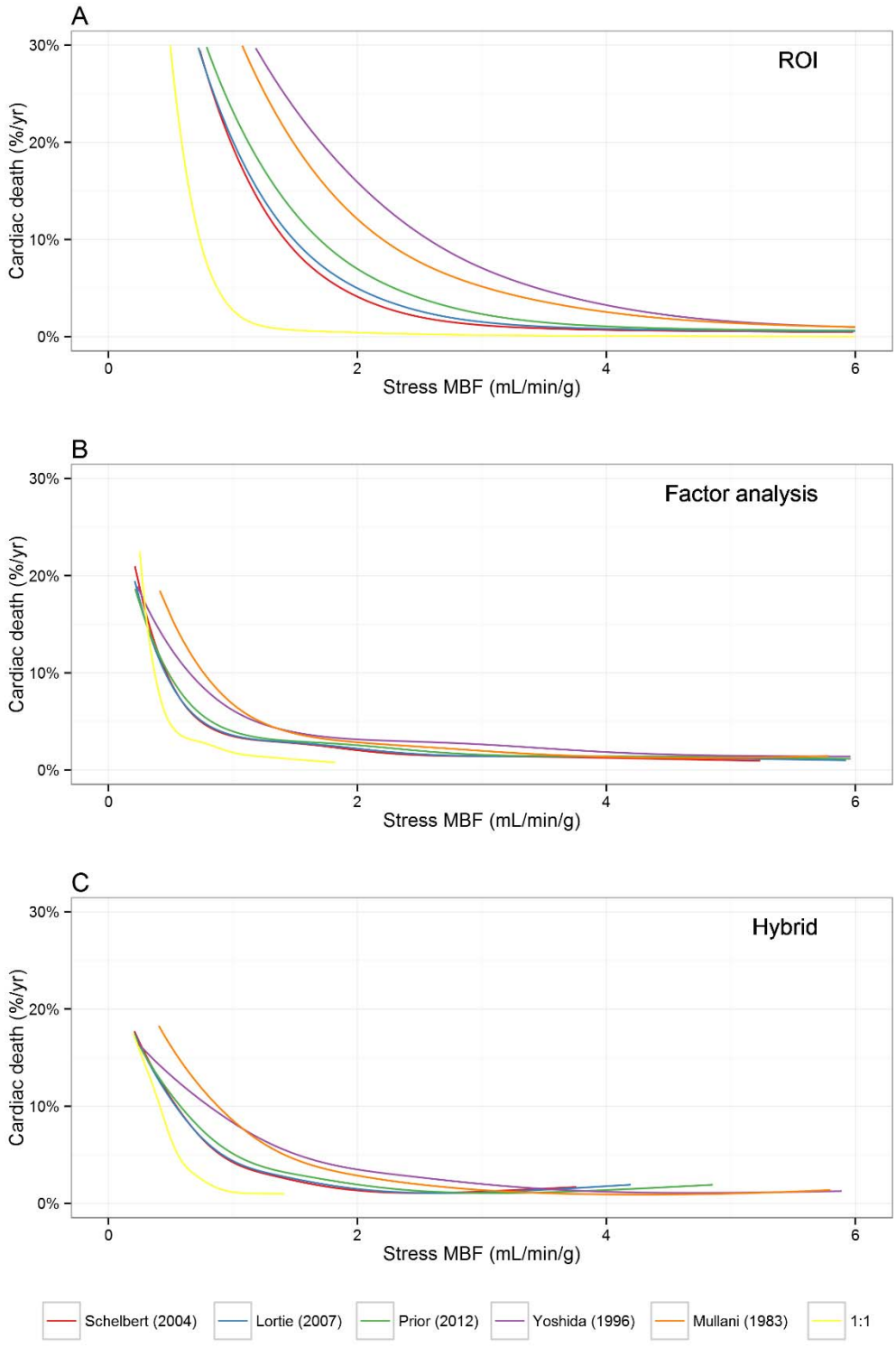

Supplemental Figure 20: Risk of Cardiac Death Versus Stress MBF Without RV Spillover Correction. Annual rate of death from cardiac causes as a function of stress MBF computed using (A) ROI, (B) factor

analysis, and (C) hybrid methods for estimation of the input function and 5 different clinically used extraction models for ^{82}Rb and 1 counterfactual model assuming 100% extraction (1:1). Curves generated using Poisson regression with smoothing splines. For this analysis no RV spillover correction was performed for any of the input function methods. In contrast, in Figure 4, RV spillover correction was performed for the factor analysis and hybrid methods.

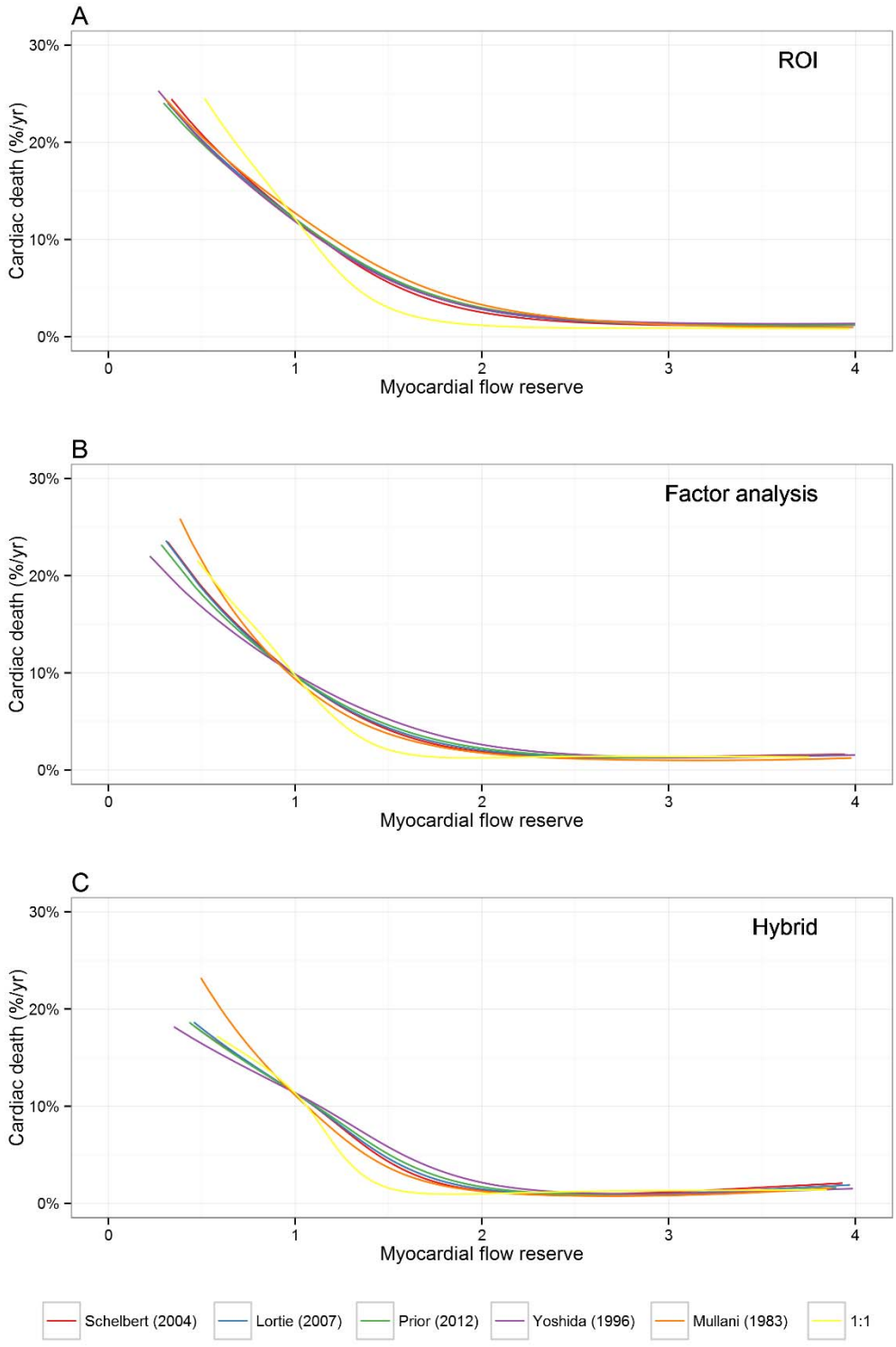

Supplemental Figure 21: Risk of Cardiac Death Versus MFR Without RV Spillover Correction. Annual rate of death from cardiac causes as a function of MFR computed using (A) ROI, (B) factor analysis, and (C)

hybrid methods for estimation of the input function and 5 different clinically used extraction models for ^{82}Rb and 1 counterfactual model assuming 100% extraction (1:1). Curves generated using Poisson regression with smoothing splines. For this analysis no RV spillover correction was performed for any of the input function methods. In contrast, in Figure 5, RV spillover correction was performed for the factor analysis and hybrid methods.

Supplemental Table 1: K_1 and k_2 for Three Input Function Methods

State	Input Function Method	K1	K2	Pearson Correlation	P-Value
Stress	ROI	1.03±0.34	0.16±0.08	0.41	<0.0001
	Factor Analysis	0.59±0.18	0.04±0.08	0.08	<0.0001
	Hybrid	0.62±0.17	0.14±0.07	0.01	0.72
Rest	ROI	0.70±0.16	0.15±0.07	0.51	<0.0001
	Factor Analysis	0.44±0.10	0.05±0.12	0.15	<0.0001
	Hybrid	0.47±0.09	0.15±0.07	-0.02	0.23

Supplemental Table 2: Values of Stress MBF and MFR Using Various Input Function Methods and Extraction Models

		Input Function Method Factor		
Measurement	**Extraction Model**	**ROI**	**Analysis**	**Hybrid**
Stress MBF	Schelbert (2004) (*7*)	2.42±0.99	1.02±0.53	1.11±0.49
	Lortie (2007) (*3*)	2.64±1.13	1.05±0.58	1.15±0.54
	Prior (2012) (*4*)	3.03±1.29	1.18±0.69	1.30±0.64
	Yoshida (1996) (*2*)	4.42±1.71	1.75±1.04	1.94±0.97
	Mullani (1983) (*8*)	4.49±2.23	1.62±0.96	1.75±0.87
MFR	Schelbert (2004) (*7*)	1.94±0.81	1.61±0.57	1.63±0.52
	Lortie (2007) (*3*)	2.04±0.90	1.65±0.62	1.68±0.57
	Prior (2012) (*4*)	2.08±0.94	1.71±0.68	1.74±0.62
	Yoshida (1996) (*2*)	2.02±0.88	1.82±0.77	1.83±0.69
	Mullani (1983) (*8*)	2.30±1.16	1.55±0.60	1.58±0.54

Values are means ± standard deviation.

Supplemental Table 3: NRI for Stress MBF and MFR Using Various Input Function Methods and Extraction Models

Measurement	Extraction Model	ROI	Factor Analysis	Hybrid
Stress MBF	Schelbert (2004) (*7*)	0.35 (0.13-0.59)	0.02 (-0.13-0.27)	0.25 (-0.06-0.46)
	Lortie (2007) (*3*)	0.35 (0.13-0.59)	0.02 (-0.13-0.27)	0.24 (-0.06-0.45)
	Prior (2012) (*4*)	0.35 (0.13-0.59)	0.02 (-0.13-0.27)	0.21 (-0.06-0.45)
	Yoshida (1996) (*2*)	0.36 (0.12-0.59)	0.04 (-0.12-0.28)	0.26 (-0.06-0.47)
	Mullani (1983) (*8*)	0.31 (0.14-0.56)	-0.06 (-0.19-0.3)	0.14 (-0.09-0.41)
	1:1	0.36 (0.12-0.59)	0.04 (-0.12-0.26)	0.26 (-0.07-0.49)
MFR	Schelbert (2004) (*7*)	0.51 (0.24-0.67)	0.35 (0.09-0.55)	0.43 (0.22-0.65)
	Lortie (2007) (*3*)	0.50 (0.24-0.66)	0.34 (0.08-0.54)	0.39 (0.23-0.64)
	Prior (2012) (*4*)	0.49 (0.24-0.66)	0.36 (0.08-0.54)	0.41 (0.22-0.64)
	Yoshida (1996) (*2*)	0.48 (0.22-0.64)	0.43 (0.13-0.59)	0.43 (0.22-0.66)
	Mullani (1983) (*8*)	0.45 (0.21-0.67)	0.25 (-0.03-0.47)	0.43 (0.18-0.63)
	1:1	0.53 (0.25-0.68)	0.32 (0.12-0.54)	0.41 (0.20-0.64)

Values in parenthesis are 95% confidence intervals. NRI is statistically significant when the 95% confidence intervals do not cross zero. NRI=net reclassification improvement.

REFERENCES

1. Weinberg IN, Huang SC, Hoffman EJ, et al. Validation of PET-acquired input functions for cardiac studies. *J Nucl Med*. 1988;29:241-247.

2. Yoshida K, Mullani N, Gould KL. Coronary flow and flow reserve by PET simplified for clinical applications using rubidium-82 or nitrogen-13-ammonia. *J Nucl Med*. 1996;37:1701-1712.

3. Lortie M, Beanlands RSB, Yoshinaga K, Klein R, DaSilva JN, deKemp RA. Quantification of myocardial blood flow with 82Rb dynamic PET imaging. *Eur J Nucl Med Mol Imaging*. 2007;34:1765-1774.

4. Prior JO, Allenbach G, Valenta I, et al. Quantification of myocardial blood flow with 82Rb positron emission tomography: clinical validation with 15O-water. *Eur J Nucl Med Mol Imaging*. 2012;39:1037-1047.

5. Gambhir SS, Schwaiger M, Huang SC, et al. Simple noninvasive quantification method for measuring myocardial glucose utilization in humans employing positron emission tomography and fluorine-18 deoxyglucose. *J Nucl Med*. 1989;30:359-366.

6. Hutchins GD, Schwaiger M, Rosenspire KC, Krivokapich J, Schelbert H, Kuhl DE. Noninvasive quantification of regional blood flow in the human heart using N-13 ammonia and dynamic positron emission tomographic imaging. *J Am Coll Cardiol*. 1990;15:1032-1042.

7. Schelbert HR. Positron emission tomography of the heart: Methodology, findings in the normal and the diseased heart, and clinical applications. In: *PET: Molecular Imaging and Its Biological Applications*. Springer New York; 2004:389-508.

8. Mullani NA, Goldstein RA, Gould KL, et al. Myocardial perfusion with rubidium-82. I. Measurement of extraction fraction and flow with external detectors. *J Nucl Med*. 1983;24:898-906.